Abstract

There is a wide interest in studying the membrane mobility of Nerve Growth Factor (NGF)* tropomyosin receptor kinase A (TrkA) at the single molecule level, in order to elucidate its diverse signaling responses related to different receptor functions. Here we present an experimental strategy based on the acyl carrier protein (ACP) tag in order to study the dynamics of the high-affinity NGF receptor TrkA in the membrane of PC12*nnr*5 cells. We present a single-particle tracking (SPT) study using highly photostable semiconductor quantum dots (Qdots) conjugated to ACP-tagged TrkA receptors. We demonstrate that ACP-TrkA shows biochemical and biological properties identical to those of its unmodified counterpart and that single receptor molecules in living cells display distinct diffusive regimes and a highly heterogeneous dynamics.

Keywords

- Acyl carrier protein
- Single particle tracking
- Semiconductor Quantum Dots
- Receptor dynamics
- TrkA

1. Introduction

The TrkA receptor (Klein et al., 1991) binds NGF with high-affinity and this process eventually leads to development and survival of sympathetic and sensory neurons, neuronal plasticity, and differentiation of central nervous system cholinergic neurons (Levi-Montalcini, 1987). TrkA is also involved in pathological situations, such as chronic pain (Ugolini et al. 2007) and Alzheimer's disease (Capsoni et al. 2010). Growing evidence points to a close relationship between neurotrophin-receptor trafficking, cellular location and signaling (Segal, 2003). More generally, membrane-receptor mobility represents a major determinant of signal transduction, between and within cells in organisms (Chung et al., 2010). Hence, the ability to accurately monitor TrkA dynamics both as isolated molecules and as part of a NGF-receptor complex represents a very powerful tool, particularly if this is performed at the single-receptor level. TrkA receptor dynamics is mainly investigated indirectly, by means of fluorescent NGF (Echarte et al., 2007). This strategy limits the study of the receptor in its activated state and possibly in the presence of $p75^{NTR}$ co-receptor, thus preventing a direct comparison between receptor mobility in the presence and absence of the ligand-dependent stimulation.

Here we present a method that makes it possible to monitor the dynamics of individual TrkA receptors in living cells. Notably, thanks to this tool it is possible to quantitatively investigate receptor dynamics independently of its ligand-binding state. To this purpose, we fused the ACP sequence (Johnsson et al., 2005) to the extracellular domain of TrkA, expressed it in TrkA-deficient PC12*nnr*5 cells, and selectively conjugated the receptors at the cell surface with Qdots in order to track them with single-

* **Abbreviations**: **NGF**, Nerve Growth Factor; **TrkA**, Tropomyosin Receptor Kinase A; **ACP**, Acyl Carrier Protein; **Qdot**, Quantum dot; **$p75^{NTR}$,** Low affinity neurotrophin receptor; **S-Qdot**, streptavidin-conjugated Qdot; **SPT**, Single Particle Tracking; **SP**, Signal Peptide; **NA**, Numerical Aperture; **ROI**, Region Of Interest; **MSD**, Mean Square Displacement.

molecule resolution. We demonstrate that (*i*) ACP-tagging fully preserves TrkA biochemical and signaling functions, including internalization of the labeled receptor upon NGF addition and that (*ii*) Qdot-conjugated ACP-TrkA receptors can be followed by SPT and display heterogeneous diffusion patterns with three major diffusion regimes: Brownian, confined and drifted. The possible biological implications of the observed dynamic behavior will be discussed.

2. Experimental

Detailed information about all the experimental parts of the work can be found in the Supplementary Data file.

2.1 Cloning- The ACP-tag was fused to rat TrkA cDNA by three sequential cloning steps. First, the TrkA signal peptide (SP) sequence (aminoacids 1-35) was PCR amplified and subcloned into pCDNA3.1(+) (Invitrogen), yielding the SP_pCDNA construct. Second, the ACP sequence was PCR amplified from the plasmid pACP-tag(m) (New England Biolabs) and inserted in the SP_pCDNA plasmid, yielding the SP_ACP_pCDNA construct. Finally, the rest of the TrkA coding sequence was PCR amplified and subcloned in the SP_ACP_pCDNA leading to the construct SP_ACP_TrkA-pCDNA (referred to as ACP-TrkA).

2.2 Western Blot- Immunoblot was performed from lysates of electroporated cells using either rabbit anti-phospho-Tyr490 (equivalent to rat Tyr499; 1:500) or mouse anti-phospho ERK 1/2 (1:1000) primary antibodies; detection was performed with anti-rabbit or anti-mouse horseradish-peroxidase-conjugated secondary antibodies (1:2500).

2.3 Immunocytochemistry and differentiation assay- Electroporated PC12*nnr*5 cells were differentiated with NGF (100 ng/ml). Immunocytochemistry was carried out with rabbit anti-TrkA primary antibody (1:100 in PBS-8% BSA) and anti-rabbit Alexa594 secondary antibody (1:250 in PBS-8% BSA).

2.4 Cell labeling with S-Qdot655- 24h post-transfected PC12*nnr*5 cells were differentiated (3-5 days; 100 ng/mL NGF). After over-night starvation, cells were biotinylated, processed and finally imaged as described (Bannai et al., 2006).

2.5 Single-molecule microscopy- Differentiated PC12*nnr*5 cells were imaged with a Leica DM6000 epifluorescence microscope equipped with an incubator chamber, an electron multiplying charge-coupled-device camera (Cascade II:512, Photometrics) and a mercury lamp (Leica), by using a 100X oil immersion objective (NA 1.46) and a Qdot655/10 optical filtercube (K32011, Leica).

2.6 Single-molecule tracking and trajectory analysis- Trajectories were built connecting detected spot positions across frames within the entire image stack (see Supplementary Data, section 2.10) and exported as a series of two-dimensional images encoding fluorescence intensity and position ($x_i(t)$; $y_i(t)$) of the individual detected spots. The center of each fluorescent spot was located by Gaussian fitting of the intensity profile and associated to an individual receptor. The S-Qdot-labeled ACP-TrkA diffusivity were quantified by analyzing the MSD curve. Only the first 25% of the MSD curve was calculated, in order to use well-averaged MSD values, and allow the fitting of models beyond the simple Brownian diffusion (see Supplementary Data, section

2.10.3).

Different types of motion can be distinguished from the time dependence of the MSD (Bannai et al., 2006). We classified trajectories into one of four different categories: (*i*) *adsorbed*, for static ACP-TrkA receptors, (*ii*) *confined*, for the case of diffusion limited by corrals or impaired by obstacles, (*iii*) *Brownian,* and (*iv*) *drifted* for trajectories where a directed motion with velocity *V* is present. The best-fitting model of the data was decided considering the reduced Chi-square $\tilde{\chi}^2$. Regardless of the specific diffusion regime underwent by the particle, it is always possible to calculate an *"average" diffusivity* $D_{1\text{-}2}$*, i.e.* the slope of the line connecting the first two MSD points (at lag-times ΔT and $2\Delta T$) as shown by Triller et al. (Triller and Choquet, 2008).

3. Results

3.1 Biochemical validation of ACP-TrkA- The ACP-TrkA fusion protein was transiently expressed by transfection into PC12*nnr*5 cells, a TrkA-defective mutant cell line derived from pheochromocytoma PC12 cells (Green et al., 1986). The phosphorylation of TrkA Tyr499 and the activation of the two downstream kinases ERK1 and ERK2 were assayed following NGF addition (Fig. 1A). The Tyr499-phosphorylation levels are enhanced in the ACP-TrkA transfected and NGF-treated PC12*nnr*5 cells (top panel, lane 3), when compared to the negative-control (lane 4). Correspondingly, phosphorylation of ERK1/2 effectors is much higher in NGF-stimulated cells (lower panel, lane 3) than in the untreated control (lane 4). Negligible phosphorylation levels of both TrkA-Tyr499 and ERK1/2 were observed in untransfected PC12*nnr*5 cells (bottom panel, lanes 1-2). These results demonstrate ACP-TrkA dependent signaling in PC12*nnr*5 cells, which are otherwise unresponsive to NGF.

3.2 ACP-TrkA induces NGF-dependent neurite outgrowth in PC12nnr5 cells- In order to check if the ACP-TrkA construct is functional and able to mediate the NGF-dependent neurite outgrowth when transiently transfected in PC12*nnr*5 cells, transfected cells were left differentiating either in presence (Fig. 1B, bottom) or absence (Fig. 1B, middle) of NGF for 96 hours. Untransfected PC12*nnr*5 cells were used as control (Fig. 1B, top). Each sample was immunostained for TrkA, to assess the actual expression of the ACP-TrkA fusion protein. As expected, the anti-TrkA antibody did not stain untransfected PC12*nnr*5 cells (Fig 1B, top panel, left) and cell morphology was not altered by NGF treatment (top panel, right), *i.e.* these cells are not responsive to NGF. Transfected cells (middle panel, left) showed anti-TrkA staining and only few of them -likely those overexpressing the construct- developed neurite-like structures in absence of NGF treatment (middle panel, right). Oppositely, ACP-TrkA transfected cells clearly showed neurite outgrowth and developed a complex network of neurites when treated with NGF (bottom panel). Thus, the ACP-TrkA construct can rescue NGF responsivity to PC12*nnr*5 cells and thus proves its full biochemical functionality.

3.3 NGF induces effective ACP-TrkA internalization - We analyzed the properties of ACP-TrkA when labeled with S-Qdots by investigating its internalization upon NGF treatment. To this purpose, we transiently transfected ACP-TrkA in CHO cells, which express neither TrkA nor the low-affinity NGF-binding receptor $p75^{NTR}$ (Zapf-Colby and Olefsky, 1998). The latter is present in PC12*nnr*5 (Deinhardt et al., 2007) and might affect the overall TrkA internalization rate upon NGF-binding. We selectively labeled the ACP-TrkA pool at the plasma membrane, by exploiting the possibility of the ACP-tag to be stained at cell surface,

via coenzyme A conjugated dyes (Johnsson et al., 2005). In particular, we covalently attached a biotin-coenzyme A conjugate to ACP-TrkA, which was further linked to Streptavidin-Qdots emitting at 655 nm. We found that untreated cells (Fig. 1C, top panel row) show prevalent S-Qdot staining at the cell outer rims, whereas in NGF-treated cells (bottom panel row) the S-Qdot fluorescence is spotted within the cell interior. The internalization level was quantified as the ratio between S-Qdot fluorescence signal in two ROIs (see Experimental and Fig.1C) : $\overline{F}_i$ (mean fluorescence from the cytoplasm) and $\overline{F}_m$ (mean fluorescence from the membrane). The box-plot shows that NGF-treated cells (blue box, n = 44) internalize labeled ACP-TrkA receptors at a much higher level compared to untreated-samples (red box, n = 36). Information on ACP-TrkA internalization pathway was obtained by carrying out colocalization studies of Cy5-labeled ACP-TrkA receptors with transferrin-Alexa 488 in living, transiently-transfected PC12*nnr*5 cells. Cells maintained at 37°C do actively internalize both labeled transferrin and ACP-TrkA receptors in the presence of NGF (Fig. 1D, green and red channels, respectively). Data showed unequivocally that the neurotrophic receptor enters early/recycling endosomes (Fig. 1D, insets 1-2).

3.4 ACP-TrkA SPT and trajectories analysis- By taking advantage of Qdot intense fluorescence, we performed SPT of ACP-TrkA receptors (Fig. 1E shows a typical distribution pattern of S-Qdots in transfected PC12*nnr*5 cells). Individual trajectories were recorded and analyzed by calculating the corresponding MSD (Fig. 2A-C). For Brownian particles, the MSD increases linearly with time. For receptors confined in a restricted area, the MSD rapidly reaches a *plateau*. Finally, for drifting receptors, the transport component dominates over the pure diffusive one (see also Supplementary Data, section 2.10.3-D). Figure 2 clearly shows that TrkA receptors display a variety of diffusive behavior types beyond the simple Brownian one (Fig. 2A and Supplementary Video Movie1.avi). Specifically, ACP-TrkA receptors can be drifting (Fig. 2B and Supplementary Video Movie2.avi) or confined (Fig. 2C and Supplementary Video Movie3.avi). MSD curves also identify particles with a more complex diffusion pattern (Supplementary Data, Fig. S1) not fitted by the previously mentioned models. These cases can result from a combination of Brownian, confined and drifting intervals.

MSD data yield the “average” diffusion coefficient $D_{1\text{-}2}$, an estimate of the receptor diffusion rate regardless of the detailed type of dynamics (Kusumi et al., 1993). Figure 2D (red curve) shows that measured $D_{1\text{-}2}$ values of ACP-TrkA receptors are distributed over four orders of magnitude from ~10^{-5} $\mu m^2 s^{-1}$ to ~0.5 $\mu m^2 s^{-1}$, thus proving that ACP-TrkA receptors present a highly heterogeneous diffusive behavior. Calculated trajectories were grouped in four different diffusive classes according to the best-fitting model. Trajectories fitted with statistically significant results ($0.005 < P\left(\tilde{\chi}^2\right) < 0.995$) were further divided into two groups corresponding to the trajectories detected in the neuritic and somatic cell compartments of the analyzed cells (Fig. 2E). In both groups, the majority of ACP-TrkA receptors were classified as confined (>70% in neurite-like structures and >78% in cell bodies); about 11-14% of particles turned out to be adsorbed to the substrate probably due to unspecific substrate-Qdot interactions. The remaining fraction of trajectories was classified into either pure-Brownian (neurites ~7%; cell somas ~5%) or drifting (neurites ~9%; cell somas ~6%) groups.

4. Discussion

In this paper we presented an ACP-tagging-based method to investigate the dynamics of single TrkA molecules in living cells. We first assessed that ACP-TrkA maintains the same functional activity of its endogenous counterpart (Fig.1). This step is

required since ACP insertion may lead to non-functional constructs (Kasai et al., 2011).

ACP-TrkA dynamics was then investigated by SPT. This technique relies on the possibility to selectively label the molecule of interest, ideally leading to few, bright detectable spots in the acquisition field. The ACP-tag ensures high labeling selectivity by conferring a unique reactivity to the protein of interest - namely, TrkA - on the cell surface. Thus only those ACP-TrkA receptors located at the cell surface could be biotinylated and labeled with S-Qdot. Multivalent S-Qdots may cross-link surface proteins and activate signaling pathways, dramatically reducing receptor mobility (Howarth et al., 2008). In order to avoid this and achieve a ratio of approximately one single S-Qdot per biotinylated ACP-TrkA receptor, we partially saturated free binding-sites using a molar excess of free biotin before performing the labeling reaction. Qdots may alter membrane trafficking dynamics (Tekle et al., 2008); however, Qdot-based labeling is exploited by many groups (Groc et al., 2007; Renner et al., 2010) that did not detect any relevant adverse effects on receptor mobility. Undoubtedly, Qdots represent the best solution presently available for SPT, also thanks to their optimal photophysical properties (*i.e.* high brightness and photostability).

MSD analysis of individual ACP-TrkA trajectories demonstrates that this receptor presents three different kinds of diffusive motions: Brownian, confined and drifted (Fig. 2A-C) and yielded the respective population (Fig. 2E) within neurites and cell-soma. Interestingly, an increase in the drifting trajectories was observed in the neuritic compartment; oppositely, confined trajectories are more frequent in the somatic cell compartment. It can be argued that Brownian movement corresponds to unguided movement at the cell surface. On the contrary the drifting pattern is suggestive of active movement on microtubules. Confined movement may correspond to receptors tethered to intracellular signaling loci. These are preliminary observations that need further investigations to be mechanistically explained.

Some of the trajectories analyzed over longer time-scales (>1 minute) showed complex MSD(τ) curves which cannot be interpreted by a single diffusion model; these trajectories could result from the composition of different regimes, (*e.g.*, see supplementary Fig. S1 and supplementary video Movie4.avi). Non-uniform dynamics might be related to plasma-membrane anisotropies and/or different signaling states, as reported previously for EGFR (Chung et al., 2010).

Interestingly, the $D_{1\text{-}2}$ distribution (Fig. 2D, red line) spans over 4 orders of magnitude. Even considering that most of the receptors with $D_{1\text{-}2}<0.001$ $\mu m^2/s$ should be considered as quasi-immobile or adsorbed, $D_{1\text{-}2}$ for non-immobilized TrkA spans almost 3 orders of magnitude; this does not change significantly if we consider any one of the considered regimes only (data not shown). Whether this heterogeneity in $D_{1\text{-}2}$ distribution reflects different cellular locations of the receptor itself, or rather is an intrinsic feature of the receptor dynamics, remains to be explored and will be the subject of future investigations.

4.1 Conclusions- We showed that the ACP-based technique offers a new perspective for studying TrkA mobility at the single-molecule level in living cells. Furthermore, our findings suggest that, while most receptors seem to be confined or to diffuse very slowly, TrkA undergoes a highly heterogeneous dynamic behavior, especially when the receptor is tracked for long times. Thanks to this tool, TrkA may be studied either in the absence or in the presence of NGF stimulation, offering a versatile way to investigate NGF-dependent effects, also exploiting the joint single-molecule tracking of the NGF ligand (Cui et al., 2007), to distinguish ligand-bound from ligand-free TrkA molecules. Additionally, it will be of interest to study how TrkA mobility can be affected in cells under different pharmacological or disease-related treatments.

5. Acknowledgements

The authors thank Dr. Marcello Ceci (European Brain Research Institute, Rome) for stimulating discussions and support. The authors disclose no financial conflict of interest.

This research was supported in part by the Italian Ministry for University and Research under FIRB No. RBLA03ER38 and by Fondazione Monte dei Paschi di Siena.

6. References

Bannai H, Levi S, Schweizer C, Dahan M, Triller A. Imaging the lateral diffusion of membrane molecules with quantum dots. Nat Protoc, 2006; 1: 2628-34.

Capsoni S, Tiveron C, Vignone D, Amato G, Cattaneo A. Dissecting the involvement of tropomyosin-related kinase A and p75 neurotrophin receptor signaling in NGF deficit-induced neurodegeneration. Proc Natl Acad Sci U S A, 2010; 107: 12299-304.

Chung I, Akita R, Vandlen R, Toomre D, Schlessinger J, Mellman I. Spatial control of EGF receptor activation by reversible dimerization on living cells. Nature, 2010; 464: 783-7.

Cui B, Wu C, Chen L, Ramirez A, Bearer EL, Li WP, Mobley WC, Chu S. One at a time, live tracking of NGF axonal transport using quantum dots. Proc Natl Acad Sci U S A, 2007; 104: 13666-71.

Deinhardt K, Reversi A, Berninghausen O, Hopkins CR, Schiavo G. Neurotrophins Redirect p75NTR from a clathrin-independent to a clathrin-dependent endocytic pathway coupled to axonal transport. Traffic, 2007; 8: 1736-49.

Echarte MM, Bruno L, Arndt-Jovin DJ, Jovin TM, Pietrasanta LI. Quantitative single particle tracking of NGF-receptor complexes: transport is bidirectional but biased by longer retrograde run lengths. FEBS Lett, 2007; 581: 2905-13.

Green SH, Rydel RE, Connolly JL, Greene LA. PC12 cell mutants that possess low- but not high-affinity nerve growth factor receptors neither respond to nor internalize nerve growth factor. J Cell Biol, 1986; 102: 830-43.

Groc L, Lafourcade M, Heine M, Renner M, Racine V, Sibarita JB, Lounis B, Choquet D, Cognet L. Surface trafficking of neurotransmitter receptor: comparison between single-molecule/quantum dot strategies. J Neurosci, 2007; 27: 12433-7.

Howarth M, Liu W, Puthenveetil S, Zheng Y, Marshall LF, Schmidt MM, Wittrup KD, Bawendi MG, Ting AY. Monovalent, reduced-size quantum dots for imaging receptors on living cells. Nat Methods, 2008; 5: 397-9.

Johnsson N, George N, Johnsson K. Protein chemistry on the surface of living cells. Chembiochem, 2005; 6: 47-52.

Kasai RS, Suzuki KG, Prossnitz ER, Koyama-Honda I, Nakada C, Fujiwara TK, Kusumi A. Full characterization of GPCR monomer-dimer dynamic equilibrium by single molecule imaging. J Cell Biol, 2011; 192: 463-80.

Klein R, Jing SQ, Nanduri V, O'Rourke E, Barbacid M. The trk proto-oncogene encodes a receptor for nerve growth factor. Cell, 1991; 65: 189-97.

Kusumi A, Sako Y, Yamamoto M. Confined lateral diffusion of membrane receptors as studied by single particle tracking (nanovid microscopy). Effects of calcium-induced differentiation in cultured epithelial cells. Biophys J, 1993; 65: 2021-40.

Levi-Montalcini R. The nerve growth factor 35 years later. Science, 1987; 237: 1154-62.

Renner M, Lacor PN, Velasco PT, Xu J, Contractor A, Klein WL, Triller A. Deleterious effects of amyloid beta oligomers acting as an extracellular scaffold for mGluR5. Neuron, 2010; 66: 739-54.

Segal RA. Selectivity in neurotrophin signaling: theme and variations. Annu Rev Neurosci, 2003; 26: 299-330.

Tekle C, Deurs B, Sandvig K, Iversen TG. Cellular trafficking of quantum dot-ligand bioconjugates and their induction of changes in normal routing of unconjugated ligands. Nano Lett, 2008; 8: 1858-65.

Triller A, Choquet D. New concepts in synaptic biology derived from single-molecule imaging. Neuron, 2008; 59: 359-74.

Zapf-Colby A, Olefsky JM. Nerve growth factor processing and trafficking events following TrkA-mediated endocytosis. Endocrinology, 1998; 139: 3232-40.

Figure captions

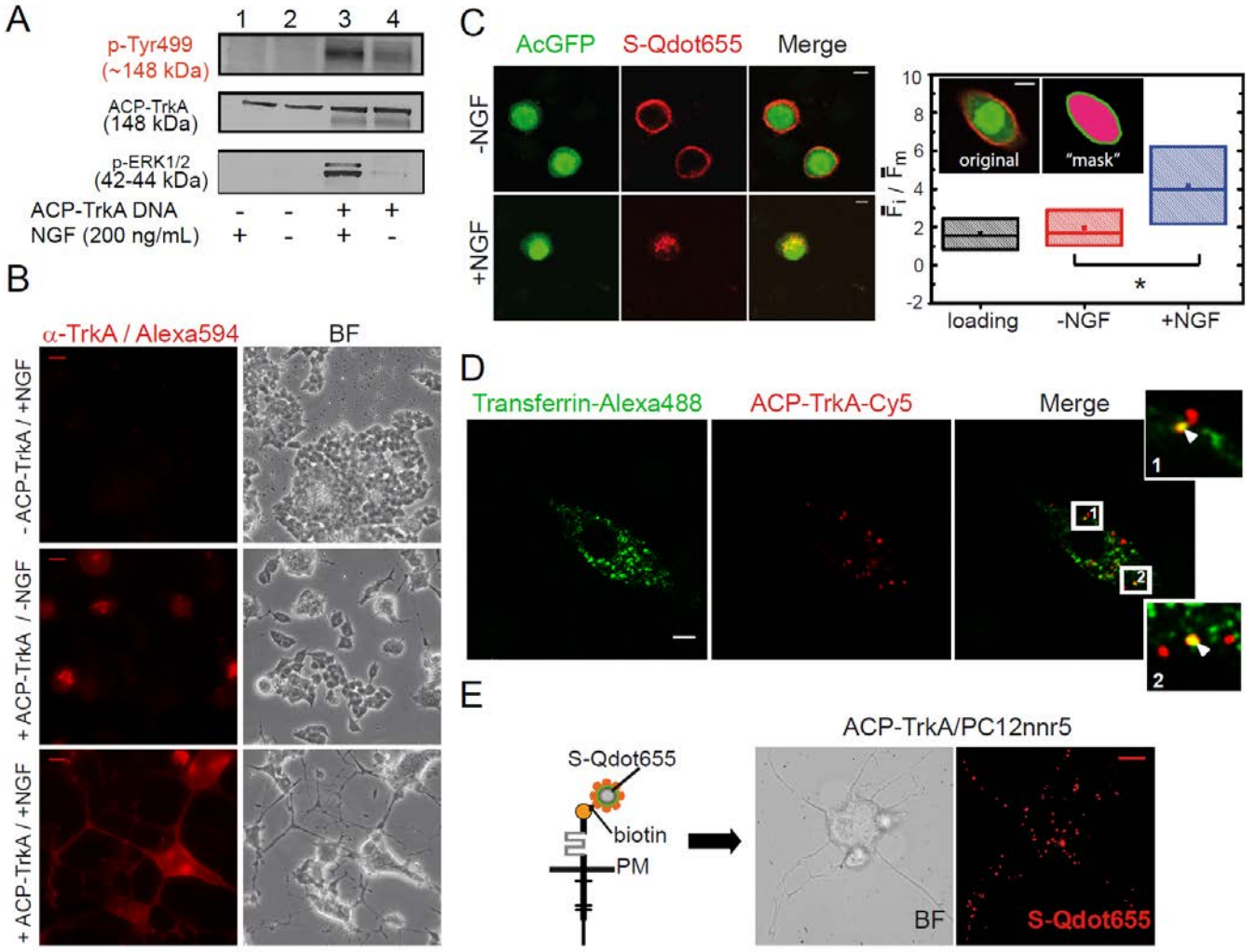

Fig. 1 *Functional validation of ACP-TrkA fusion protein.* (A) Western blot showing ACP-TrkA response to NGF in PC12*nnr*5 cells. Autophosphorylation of ACP-TrkA Tyr499 residues (top panel, lane 3) and activation of ERK1/2 effectors (lower panel, lane 3). (B) NGF-dependent neurite outgrowth in ACP-TrkA transfected PC12*nnr*5 cells. Electroporated cells (+ACP-TrkA, middle and bottom panels) are stained with anti-TrkA antibody (Alexa594 fluorescence channel, red). Bars: 50 μm. (C) Internalization assay of ACP-TrkA receptors conjugated to S-Qdots in CHO cells. Untreated (-NGF) and treated cells (+NGF) are shown in the upper and lower panel rows, respectively. Internalized *vs* surface-localized receptor pools ($\overline{F}_i / \overline{F}_m$) are box-plotted for loading-control (black box, $n_{loading}$=7), untreated (-NGF, red box, n_{-NGF}=38) and treated samples (+NGF, blue box, n_{+NGF}=44). ***P* < 0.001, Mann-Whitney test. Average ratios (■) are displayed; standard deviation (SD) and median value of each dataset correspond to box heights and central line, respectively. Bars: 10 μm. (D) Colocalization between Transferrin-Alexa 488 (green) and ACP-TrkA conjugated to Cy5-CoA (red) in living PC12*nnr*5 cells. Yellow spots (inset arrowheads) show colocalizing features. Bar: 5 μm. (E) S-Qdots-labeled ACP-TrkA receptors (red spots) distribution pattern in differentiated PC12*nnr*5 cells. Bar: 10 μm.

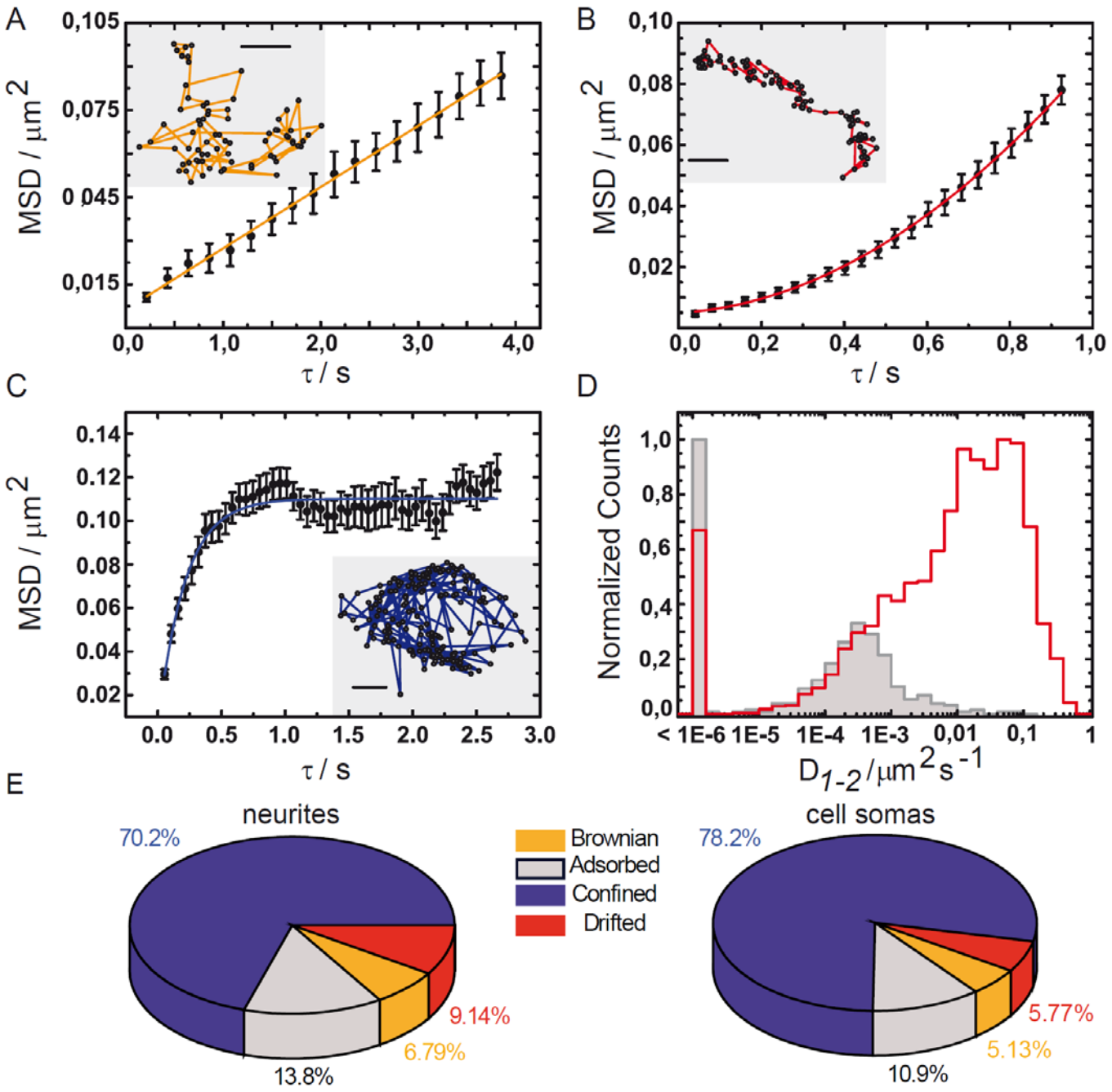

Fig.2 *MSD analysis of particle trajectories.* (A-C) MSD *vs* lag-time (τ) plots for trajectories (insets) epitomizing three diffusive regimes associated to individual ACP-TrkA receptors: (A) Brownian (yellow curve), (B) drifted (red curve) and (C) confined (blue curve) regimes. Bar: 0.16 µm (1 pixel). (D) Global distribution of average diffusivities ($D_{1\text{-}2}$) associated to each single trajectory (red curve) and $D_{1\text{-}2}$ distribution of S-Qdot655 immobilized to the glass surface (gray curve). The bin "<1E-6" includes negative values for $D_{1\text{-}2}$, mostly arising from cases where the uncertainty is higher than the absolute value. (E) Trajectory classification in neuritic and somatic cell compartments. Numbers of trajectories classified as Brownian (yellow), drifted (red), confined (blue) and adsorbed (gray) by a fit with $0.005 < P\left(\tilde{\chi}^2\right) < 0.995$ are plotted as percentages.